The Astrophysical Journal Letters, 729:L18 (4pp), 2011 March 10 doi:10.1088/2041-8205/729/2/L18

OBSERVATIONS OF SAUSAGE MODES IN MAGNETIC PORES

R. J. Morton[1], R. Erdélyi[1], D. B. Jess[2], and M. Mathioudakis[2]
[1] Solar Physics and Space Plasma Research Centre (SP^{2}RC), University of Sheffield, Hicks Building, Hounsfield Road, Sheffield S3 7RH, UK; R.J.Morton@sheffield.ac.uk
[2] Astrophysics Research Center, School of Mathematics and Physics, Queen's University, Belfast BT7 1NN, UK; Robertus@sheffield.ac.uk
Received 2010 October 15; accepted 2011 January 3; published 2011 February 14

ABSTRACT

We present here evidence for the observation of the magnetohydrodynamic (MHD) sausage modes in magnetic pores in the solar photosphere. Further evidence for the omnipresent nature of acoustic global modes is also found. The empirical decomposition method of wave analysis is used to identify the oscillations detected through a 4170 Å "blue continuum" filter observed with the Rapid Oscillations in the Solar Atmosphere (ROSA) instrument. Out of phase, periodic behavior in pore size and intensity is used as an indicator of the presence of magnetoacoustic sausage oscillations. Multiple signatures of the magnetoacoustic sausage mode are found in a number of pores. The periods range from as short as 30 s up to 450 s. A number of the magnetoacoustic sausage mode oscillations found have periods of 3 and 5 minutes, similar to the acoustic global modes of the solar interior. It is proposed that these global oscillations could be the driver of the sausage-type magnetoacoustic MHD wave modes in pores.

Key words: plasmas – Sun: photosphere – waves

1. INTRODUCTION

The solar atmosphere is a highly dynamic magnetized plasma containing a large array of distinct structures that are defined by magnetic inhomogeneities. Each of these structures is able to support a wide variety of oscillatory magnetohydrodynamic (MHD) modes. Over the last 50 years there has been a steady increase in the number of observations of oscillatory phenomena in the solar atmosphere being reported (for latest reviews see, e.g., Banerjee et al. 2007; De Moortel 2009; Zaqarashvili & Erdélyi 2009; Mathioudakis et al. 2011) showing that waves and oscillations are ubiquitous in the solar atmosphere. The increase in observations coincides with the continuous improvement of space- and ground-based observing technology allowing unprecedented spatial and temporal resolution.

This high spatial and temporal resolution permits detailed investigation of some of the Sun's smallest, currently detectable magnetic features. One such feature is magnetic pores that have diameters ranging from 1 to 6 Mm. The pores are regions of intense magnetic fields (∼1700 G) first visible in the photosphere and expanding as they reach chromospheric heights. Pores show highly dynamic behavior due to a constant buffeting from the convective motion of granules at the photospheric level (Sobotka 2003; Sankarasubramanian & Rimmele 2003). There have recently been observations of photospheric structures experiencing a vortex style motion which could act as a driver for a wide variety of waves and oscillations (Bonet et al. 2008). These waves and oscillations may be able to propagate upward through the various layers in the lower solar atmosphere along the length of the pore, which itself acts as an MHD waveguide. The majority of these waves will be reflected at the transition region due to the steep gradients in sound or Alfvén speeds, the minority, however, will make it into the corona. The transmitted portion of the waves may be relevant for MHD wave heating or magnetoseismology of the solar corona (see, e.g., Klimchuk 2006; Taroyan & Erdélyi 2009). One of the exciting new discoveries associated with magnetic elements in the lower solar atmosphere is evidence for torsional Alfvén waves (Jess et al. 2009) which has, historically, been difficult to detect. Would pores be able to support the other magnetoacoustic modes? If yes, would these modes be sausage or kink? We answer these questions in the current Letter.

The nature of MHD waves in sunspots and pores has been extensively investigated, where the sunspots are modeled as thin, gravitationally stratified flux tubes (Roberts & Webb 1978; Roberts 1992). The seminal theory of Edwin & Roberts (1983) describing waves in a straight, magnetic cylinder, which has been applied extensively to coronal oscillations, was also derived for photospheric conditions. This last aspect is somewhat neglected and has only received limited attention although offering equally rich physics and opportunity for solar magnetoseismology as its coronal application. Dispersion diagrams for the photosphere (see, e.g., Edwin & Roberts 1983; Erdélyi & Fedun 2007, 2010) clearly show the nature of the waves supported by a photospheric waveguide. Perhaps more relevant to waves in pores are the dispersion diagrams presented in Evans & Roberts (1990).

The oscillations in the lower solar atmosphere, e.g., sausage, kink, etc., are thought to be driven by the granular buffeting (Evans & Roberts 1990) and the vortex motion (Kitiashivili et al. 2011), so pores are a good candidate for the observation of this oscillatory mode because of their compact structure. A further postulated driver maybe *p*-modes or other magnetoacoustic gravity waves which propagate within the solar interior (Dorotovič et al. 2008). The main feature of the sausage mode (both fast and slow) is the periodic fluctuation of the cross-sectional area of the waveguide (see, e.g., Edwin & Roberts 1983 for cylindrical and Erdélyi & Morton 2009 for elliptical waveguides). Neither Alfvén nor fast/slow kink or fluting oscillations would show evidence of perturbations of the cross-section of the waveguide. The change in the area of the cross-section caused by the sausage motion is also associated with periodic fluctuations in density and temperature within the waveguide.

Up until recently it has been almost impossible to find evidence for periodic change in cross-sections of waveguides (in any layer of the solar atmosphere), which indicates the presence of sausage oscillations. This is due to the limitations of the spatial resolution of many observing instruments. A number of earlier observations have, however, attempted to identify

the signature of sausage oscillations via the indirect detection of intensity oscillations, e.g., using Doppler shifts (Taroyan et al. 2007; Erdélyi & Taroyan 2008) or periodicities in X-ray emission (e.g., Nakariakov et al. 2003; Aschwanden et al. 2004) in the solar corona. To our knowledge, the first reported periodic oscillations in pore size were by Dorotovič et al. (2008), who observed periods from 20 minutes to 70 minutes in a photospheric pore with the Swedish Solar Telescope (SST). However, no intensity information was provided. We present here observations of sausage oscillations in a pore detected using the Rapid Oscillations in the Solar Atmosphere (ROSA) instrument. The observations are in both pore size and intensity in the best cases and solely in pore size in other cases. The periods of the oscillations range between 30 s and 450 s and do not have constant frequency suggesting continual evolution of the pore due to dynamic behavior.

2. OBSERVATIONS AND DATA REDUCTION

One new and exciting ground-based setup is the ROSA instrument which provides high spatial (100 km, 2 pixel) and temporal (0.03 s) resolutions. ROSA is situated at the Dunn Solar Telescope and further details of the experimental setup and operation of ROSA are given in Jess et al. (2010). ROSA is able to observe at multiple wavelengths allowing the investigation of the magnetic connection between the various layers of the lower solar atmosphere from deep photosphere to the upper chromosphere.

2.1. Data

The data used here were taken by ROSA at 15 : 24 UT on the 2008 August 22. A group of five magnetic pores, shown in Figure 1, were observed continually by ROSA for around 1 hr and 7 minutes with a 50 Å wide filter centered at 4170 Å. The pores were formed before the observations began and all are still present in the final image of the observing run. The 4170 Å blue continuum filter samples the lower photosphere. The spatial sampling is $0\farcs069$ pixel^{-1}, giving a 2-pixel spatial resolution of $0\farcs138$ (or 100 km) with an overall field of view of 50,200 × 50,100 km^2. The cadence obtained for this filter during the ROSA observing sequence was 0.2 s. The initial observations were processed through the ROSA data reduction pipeline which removed dark current, readout noise, camera inconsistencies, and variable light levels across the incident beam. To improve image quality, the speckle reconstruction method was used with a ratio of 64:1 (Wöger et al. 2008). After processing, the cadence of the observations was reduced to 12.8 s. Intensities are normalized to the mean background value.

2.2. Analysis

The pores are observed close to disk center, and assuming that a pore is a waveguide which extends upward into the solar atmosphere with a base in the photosphere, the line of sight is near perpendicular to the cross-section of the waveguide. This is ideal when searching for the periodic fluctuation in the area of the cross-section. Images of the pore show it is distinctly non-circular in cross-section and movies of the magnetic pore reveal that it is highly dynamic. At present, there is no such theory describing waveguides with a complicated, non-symmetric geometry, and dynamic behavior. Waves in more complicated models should still retain the same basic properties (see, e.g., Ruderman 2003) so the approximation of a circular cross-section provides an adequate representation of the pore.

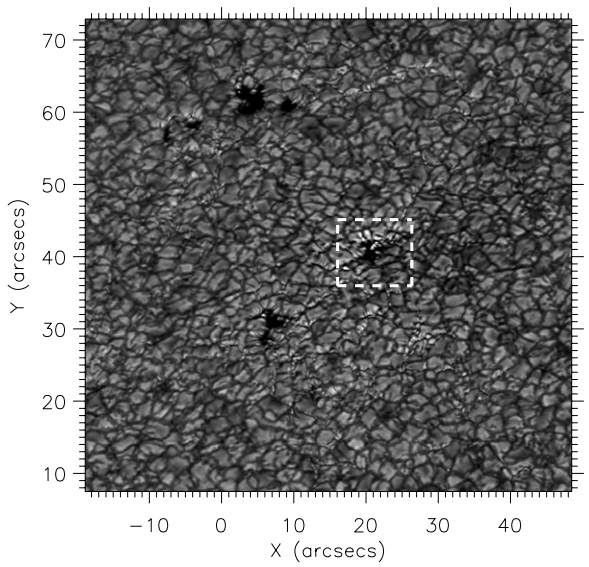

Figure 1. Field of view observed by ROSA on 2008 August 22. Boxed areas highlight pore in which oscillations are present.

The periodic change in the area of the cross-section is also accompanied by a periodic variation in intensity, which should be 180° out of phase with the change in cross-sectional area for the sausage mode.

The method used for obtaining the pore size is as follows. First, we find the median value and variance of the intensity of the whole field of view in each frame. A "box" is placed around each of the pores, large enough so that the pore is contained within the box at all times. The area of the pore is then defined as being the number of pixels with a value of intensity 3σ less than the median value of intensity, providing a 99% confidence level that the dark pore pixels are contoured.

The data representing the size of the pore are then analyzed using Empirical Mode Decomposition (EMD). This is a powerful tool that is capable of resolving non-stationary and nonlinear time series. The theory is described in Huang et al. (1998) with excellent examples of applications to solar phenomena given in Terradas et al. (2004). EMD can overcome some of the problems associated with other analysis methods (e.g., wavelet analysis) and is suitable to decompose the time series into a finite number of Intrinsic Mode Functions (IMFs). The IMFs represent the different timescales of variations in the original times series. To determine whether a sausage oscillation is present, a direct comparison between IMFs of intensity and pore size with similar timescales is performed. This shows clearly out of phase behavior. A distinct sign of sausage oscillations is when periodic phenomena in cross-section and intensity are almost 180° out of phase. We shall refer to such a signal as a strong signal. Another, although not quite as distinct, signal is when periodicities in pore size do not match with any intensity variations. In such a case, we can only assume that the expected "out of phase" intensity signal has been hidden by another effect that modifies the intensity. This will be referred to as a weak signal in the following analysis. All signals will also have to be longer than $\sqrt{2}P$ to be considered as a real oscillation. The phase information is important for finding out of phase intensity and pore size oscillations. Unless comparisons can be made between the individual time series of intensity and pore size to compare the phases, then it is virtually impossible to identify whether the periodic oscillations in pore size are due to background intensity changes or the

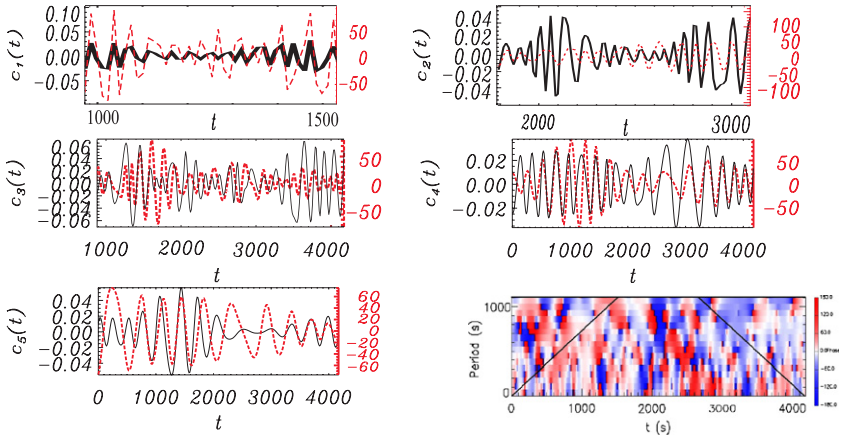

Figure 2. Shown is a direct comparison between IMF components of intensity (black solid lines) and pore size (red dashed lines). The intensity is normalized with respect to the background mean value and the pore size is measured in pixels. Last panel shows a wavelet phase plot comparing the pore size and intensity time series. The solid black line is the cone of influence.

Table 1
Periods of Identified Oscillations

IMF	Strength	Period (s)	Start time (s)	Duration (s)
c_1	Strong	30 ± 13	1200	100
c_2	Weak	102 ± 30	1900	800
c_3	Weak	140 ± 13	1700	400
	Strong	134 ± 13	2100	250
	Weak	126 ± 40	2350	1800
c_4	Weak	180 ± 13	0	375
	Weak	281 ± 18	1700	750
c_5	Weak	447 ± 13	1600	1350

sausage mode. The EMD method allows an inspection of the different timescales associated with the initial time series and proves an ideal tool for analysis. We, however, apply the wavelet method to produce phase diagrams and compare to EMD results as control.

3. OSCILLATIONS IN PORES

The pore under consideration is located in the dashed box centered at (15, 48) arcsec in Figure 1. The area is calculated with a confidence value of 3σ, i.e., 99% confidence. The average size of the pore is 536 pixels, which is roughly 1.36×10^6 km^2.

The IMFs are found for the average intensity per unit area and pore size time series and both time series reduce to eight IMF components plus the trend. The IMFs have approximate characteristic periods <100 s, 100 s, 150 s, 250 s, and 400 s for IMFs c_1 to c_5. They have also been compared to wavelet plots of the two time series and the IMF components have periods that agree well with the periods that have significant power in the wavelets.

In Figure 2 (top panels), we show a comparison between the IMF components c_1 and c_2 of pore size (red dashed lines) and average intensity per unit area (solid black lines) for a small section of the time series. Figure 2 also shows a comparison of the c_3, c_4, and c_5 components of intensity and pore size for the entire time series. The different oscillatory signals found are summarized in Table 1. It can be seen that the strong signals only last for 2–3 periods. The oscillations here have an amplitude of 20–60 pixels which corresponds to a 5×10^4 to 1.5×10^5 km^2 increase in area, which is around 4%–12% of the average pore area. The small amplitude of the oscillation suggests that the sausage waves that we observe here are linear in nature. To confirm the evidence for the sausage oscillations found in the comparison of the IMF components, we compare the two time series using cross wavelet analysis (see, e.g., Grinsted et al. 2004). We calculate the phase difference of the two time series in Figure 2 (bottom right panel). It can be seen that the areas showing the strongest out of phase behavior correspond to the periods and events identified in the IMFs. Strong out of phase behavior can also be seen for modes with (500 s), however, in the IMFs the oscillatory features did not last for longer than $\sqrt{2}P$ so were not included in Table 1.

4. WHICH MODE

When it comes to determining which mode each period in Table 1 corresponds to, i.e., fast or slow, we require more information. This is due to the plasma-β being close to 1 and the periods of the fast/slow modes are not as distinct as, say, in the corona. Due to the lack of velocity information, we are also unable to determine whether the observed oscillatory signatures are standing or propagating modes. Assuming the pore is a straight, finite flux tube with a uniform cross-section situated between the photosphere and the transition region, then standing modes can be set up with the transition region acting as a reflector (see, e.g., Malins & Erdélyi 2007). Typical values for pores are $T_i = 4000$ K inside the pore, $T_e = 6000$ K outside the pore, $B = 2$ kG, $\rho = 10^{-8}$–10^{-7} g cm^{-3}. These give values of $v_A = B/\sqrt{(\mu_0 \rho)} = 17$–$56$ km s^{-1}, $c_s = \sqrt{(\gamma T/\tilde{\mu})}$ hence $c_{si} = 5.8$ km s^{-1}, and $c_{se} = 7$ km s^{-1}, where $\mu_0 = 4\pi$, $\gamma = 5/3$, and $\tilde{\mu} = 0.6$. The phase speed of the slow mode is close to the tube speed which has estimated value, $c_T = 5.5$ km s^{-1}, whereas the fast mode has a phase speed close to c_e (see, Evans & Roberts 1990).

The period of the standing modes is given by $P \approx 2L/nc_{ph}$, where L is the tube length and $n = 1, 2, \ldots$ is the harmonic mode number. For fundamental standing modes ($n = 1$) to occur between the transition region and the photosphere (where $L \sim 2$ Mm) would then require periods of $P_f \sim 550$ s for fast modes and $P_s \sim 660$ s for slow modes. Higher harmonics, i.e., $n = 2, 3, 4, \ldots$, would have periods roughly $1/2, 1/3, \ldots$, the value of the fundamental, hence some of the periods observed here could be one of the higher harmonics, e.g., $P_f = 275$ s for $n = 2$, which is approximately the period seen in c_4. We suggest that the observed periods are

more likely to correspond to propagating modes, however, further information is required before a definite statement can be made.

A comment should be made here: the assumption that the tube is straight is a highly ideal assumption. The cross-section of the flux tube is actually expected to be expanding with height. Also, gravitational stratification plays a significant role in determining the density structuring in flux tubes located at the photosphere and should also be taken into account (Luna-Cardozo et al. 2011). Both of these effects also alter the ratio of the periods, e.g., $P_1/P_2 \neq 2$.

5. DISCUSSION

Observational evidence has been provided for examples of sausage oscillations in magnetic pores with a range of periods from ∼50 to ∼600 s. To our knowledge, this is only the second reported observation of oscillatory behavior in the area of a magnetic waveguide after Dorotovič et al. (2008). However, here we have a higher cadence allowing wave phenomena occurring on much shorter timescales to be resolved. Our observations also provide intensity information about the interior plasma of the pore, where oscillatory behavior is also seen.

The oscillatory phenomena were identified using a relatively new technique (at least to solar applications) known as EMD. Direct comparison between intensity IMFs and pore size IMFs allowed the identification of out of phase oscillatory signatures, indicating the presence of sausage oscillations. This was supported by calculation of the relative phase between the two time series. This method highlights the difficulties in obtaining a clear signal of sausage oscillations by measuring the cross-sectional area of the waveguide. Periodic changes in pore size can be related to periodic behavior in intensity (i.e., in phase periodic behavior with similar power). Using a method like wavelet analysis alone would not allow the comparison of the phases of intensity and pore size without ambiguity. Hence, wavelet analysis alone could lead to false detections of sausage modes.

Only a few sections in the various IMFs provided a clear signal of sausage oscillations, were the oscillation in pore size and intensity in the pore are out of phase by 180°. The other signals in Table 1 show oscillations in pore size that are not identified with a change in intensity, hence are a somewhat weaker signal of sausage oscillation. The periodic phenomena in intensity can most likely be attributed to global acoustic modes which are omnipresent in the photosphere and are found both inside the pore and in the surrounding granules and have a wide range of periods from tens of second to tens of minutes (see, e.g., Jess et al. 2007).

Due to the omnipresent nature of the global acoustic oscillation in the surrounding granules, it is proposed that the main driver for these oscillations is the global acoustic mode. The periods found mainly correspond to the 3 and 5 minute global modes that have been numerously reported, adding further strength to the argument. The question of whether the detected modes are standing or propagating remains unanswered due to the lack of velocity data, which could have answered this. A plausible suggestion that the oscillations were standing modes between the photosphere and the transition region would lead to the suggestion that the observed modes are higher harmonics of the fundamental standing mode.

The authors thank J. Terradas for providing the EMD routines used in the data analysis. R.E. acknowledges M. Kéray for patient encouragement. The authors are also grateful to NSF, Hungary (OTKA, Ref. No. K67746) and the Science and Technology Facilities Council (STFC), UK for the financial support they received. Observations were obtained at the National Solar Observatory, operated by the Association of Universities for Research in Astronomy, Inc. (AURA), under agreement with the National Science Foundation. We thank the technical staff at DST for their help and support during the observations.

REFERENCES

Aschwanden, M. J., Nakariakov, V. M., & Melnikov, V. F. 2004, ApJ, 600, 458
Banerjee, D., Erdélyi, R., Oliver, R., & O'Shea, E. 2007, Sol. Phys., 246, 3
Bonet, J. A., Márquez, I., Sánchez Almeida, J., Cabello, I., & Domingo, V. 2008, ApJ, 687, L131
De Moortel, I. 2009, Space Sci. Rev., 149, 65
Dorotovič, I., Erdélyi, R., & Karlovský, V. 2008, in IAU Symp. 247, Waves & Oscillations in the Solar Atmosphere: Heating and Magneto-Seismology, ed. R. Erdélyi & C. A. Mendoza-Briceño (Cambridge: Cambridge Univ. Press), 351
Edwin, P. M., & Roberts, B. 1983, Sol. Phys., 88, 179
Erdélyi, R., & Fedun, V. 2007, Sol. Phys., 246, 101
Erdélyi, R., & Fedun, V. 2010, Sol. Phys., 263, 63
Erdélyi, R., & Morton, R. J. 2009, A&A, 494, 295
Erdélyi, R., & Taroyan, Y. 2008, A&A, 489, L49
Evans, D. J., & Roberts, B. 1990, ApJ, 348, 346
Grinsted, A., Moore, J. C., & Jevrejeva, S. 2004, Nonlinear Process. Geophys., 11, 561
Huang, N. E., et al. 1998, Proc. R. Soc. A, 454, 903
Jess, D. B., Andić, A., Mathioudakis, M., Bloomfield, D. S., & Keenan, F. P. 2007, A&A, 473, 943
Jess, D. B., Mathioudakis, M., Christian, D. J., Keenan, F. P., Ryans, R. S., & Crockett, P. J. 2010, Sol. Phys., 261, 363
Jess, D. B., Mathioudakis, M., Erdélyi, R., Crockett, P. J., Keenan, F. P., & Christian, D. J. 2009, Science, 323, 1582
Kitiashivili, I. N., Kosovichev, A. G., Mansour, N. N., & Wray, A. A. 2011, ApJ, 727, L50
Klimchuk, J. A. 2006, Sol. Phys., 234, 41
Luna-Cardozo, M., Verth, G., & Erdélyi, R. 2011, A&A, submitted
Malins, C., & Erdélyi, R. 2007, Sol. Phys., 246, 41
Mathioudakis, M., Jess, D. B., & Erdélyi, R. 2011, Space Sci. Rev., submitted
Nakariakov, V. M., Melnikov, V. F., & Reznikova, V. E. 2003, A&A, 412, L7
Roberts, B. 1992, in NATO ASIC Proc. 375, Sunspots: Theory and Observations, ed. J. H. Thomas & N. O. Weiss (Dordrecht: Kluwer), 303
Roberts, B., & Webb, A. R. 1978, Sol. Phys., 56, 5
Ruderman, M. S. 2003, A&A, 409, 287
Sankarasubramanian, K., & Rimmele, T. 2003, ApJ, 598, 689
Sobotka, M. 2003, Astron. Nachr., 324, 369
Taroyan, Y., & Erdélyi, R. 2009, Space Sci. Rev., 149, 24
Taroyan, Y., Erdélyi, R., Wang, T. J., & Bradshaw, S. J. 2007, ApJ, 659, L173
Terradas, J., Oliver, R., & Ballester, J. L. 2004, ApJ, 614, 435
Wöger, F., von der Lühe, O., & Reardon, K. 2008, A&A, 488, 375
Zaqarashvili, T. V., & Erdélyi, R. 2009, Space Sci. Rev., 149, 355